NMR relaxation studies of electronic structure in $NbSe_3$

Jianhui Shi and Joseph H. Ross, Jr.
Department of Physics, Texas A&M University, College Station, Texas 77843
(Received 16 September 1991)

NMR spin-lattice relaxation measurements of the ^{93}Nb resonance for each Nb site were performed on an aligned, multicrystalline $NbSe_3$ sample at different temperatures. Results are associated with local electron densities of states for each of the three crystallographic sites, demonstrating Fermi-surface changes associated with the two charge-density-wave phase transitions. The most significant Fermi-surface changes occur for the yellow and orange crystallographic sites, at the high- and low-temperature phase transitions, respectively. The third site, however, is found to be noninsulating. A comparison is made to band theory and other experimental results.

I. INTRODUCTION

Nobium triselenide, $NbSe_3$, which has been studied extensively in recent years,[1–4] is an anisotropic quasi-one-dimensional metal possessing two incommensurate charge-density waves (CDW's). A number of unusual phenomena observed in this material are associated with the occurrence of these two apparently independent CDW's with onset temperatures of 59 and 144 K. Important electrical properties including non-Ohmic current-voltage characteristics,[5] magnetic effects,[6] and electrochemical effects[7] have aroused a great deal of interest. However, some of the electronic structure properties responsible for these features remain unclear, and our studies address this key question by using NMR spectroscopy techniques.

The crystal structure of $NbSe_3$ comprises infinite stacks of trigonal prisms of selenium atoms within the monoclinic crystal, with niobium atoms located at the center of the prisms. Each unit cell contains three inequivalent types of chain which have been labeled "orange," "red," and "yellow" by Wilson,[8] or also referred to as I, II, and III, respectively. In 1979, Wilson[8] proposed a simple conjecture that the red site loses all electrons to the orange site and the yellow site leaving one-quarter-filled bands on both the orange and yellow sites at room temperature. In this model, the red site is insulating and diamagnetic, and charge-density waves at 59 and 144 K appear on the orange site and the yellow site, respectively.

In recent years, band-structure calculations have been performed by several groups using different methods.[9–13] The results conflict as to the number of bands crossing the Fermi surface, assignment of a band to a well-defined type of chain, and whether or not the red site is really insulating. Shima and Bullett[9,11] show that the Fermi level crosses five bands and the red site is not completely empty of d electrons. Shima also proposed that the red site and the orange site are equivalent. But the recent calculation of Canadell *et al.*[14] indicates that the Fermi level crosses four bands, the red site is insulating, the CDW occurs on the yellow site, and below 59 K the remaining metallic electrons come from a partially three-dimensional band localized on the orange site.

Previous NMR experimental results[4,15] show that the yellow and the orange central lines are broadened below 145 K and below 59 K, respectively, while the red line is unaffected. Also the quadrupole structure disappears at 77 K for the yellow site and at 4.2 K for the orange site,[16] which seems to indicate that the low-temperature CDW is localized on the orange site while the high temperature CDW is localized on the yellow site. But recent scanning-tunneling-microscopy (STM) measurements[17] show quite a different picture in which the low-temperature CDW is located not only on the orange site but also on the red site, with charge modulations of nearly equal amplitude on both sites. All three sites show CDW modulation amplitudes of comparable strength. Thus the electronic distribution in $NbSe_3$ still remains controversial.

High-resolution NMR provides a crucial local microscopic probe for electronic structure studies. The aim of our experiment is to relate NMR relaxation measurements to the electronic configuration and the nature of the low-temperature phases. In this paper we present the spin-lattice relaxation (T_1) measurements for each individual ^{93}Nb site at 292, 77, and 4.2 K. These measurements are such that it is possible to study separately the effect of each CDW, since 77 and 4.2 K are well below the transitions at 145 and 59 K, respectively. We show how the metallic electron density and its change due to the electronic phase transitions in $NbSe_3$ are directly related to the T_1.

II. EXPERIMENTAL METHODS AND RESULTS

The hairlike $NbSe_3$ crystals used in our experiments were grown in our laboratory by vapor transport methods as described by Meerschaut and Rouxel.[18] Our crystals are of good electrical quality as characterized by the CDW conduction threshold (sharp minimum CDW motion threshold of approximately 150 mV/cm at 120 K). For high-resolution NMR spectra, a multicrystalline $NbSe_3$ sample was prepared by carefully aligning hairlike crystals in such a way that the long crystal axes are all parallel to each other. These ribbon-shaped monocrystals are attached to substrates by vacuum grease, and separated by layers of a low-loss microwave composite. We constructed a sample with 10 layers of crystal sealed

 ©1992 The American Physical Society

in Stycast, with dimensions of 0.45″×0.7″×0.06″. The sample contains approximately 200 crystals, sufficient to obtain an observable signal in our apparatus. Note that this is a sample different from the ones used for previous NMR studies by one of us.[19]

A homemade pulsed fast-Fourier-transform (FFT) NMR spectrometer with quadrature detection and high averaging speed was used in our measurements. We worked at frequencies near 93.610 MHz for ^{93}Nb. A superconducting magnet was used in our experiment at a magnetic field of 8.98 T, calibrated using the resonance of ^{79}Br in KBr powder. For all measurements the static field was along the *b* crystal axis. We put 8-W of transmitter power into the probe, which made the rotating H_1 field roughly 23 G. For 77- and 4.2-K measurements, we immersed the sample in liquid nitrogen and liquid helium, respectively, while we carried out the measurements for temperatures between 4.2 and 77 K via regulated helium flow.

A. Line shapes

Due to electric quadrupole coupling, the NMR spectra of ^{93}Nb ($I=\frac{9}{2}$) are composed of nine lines per site, so that the three inequivalent Nb sites in $NbSe_3$ result in 27 different lines. Our measurements concern the central transition, which is the ($m=\frac{1}{2}$ to $-\frac{1}{2}$) line, and which is the strongest due to the lack of first-order quadrupole broadening. The shape of the central lines above 77 K has already been studied extensively.[15] In this study, we observed the central-transition spectrum for each Nb site at temperatures above and below the two CDW transitions at 145 and 59 K. Spectra from several temperatures are exhibited in Fig. 1. Site identification for these spectra in this work is the same as described previously.[4,15]

^{93}Nb spectra taken near the 59-K transition temperature clearly show a sudden linewidth change for the yellow site at 59 K, in addition to the broadening at 145 K. This implies some involvement of the yellow site in the low-temperature transition, contrary to previous expectations. The yellow linewidth [full width at half maximum (FWHM) of the broadened line] is plotted in Fig. 2. A small broadening of the orange central line is also observed below the low-temperature transition. By contrast, no change in the red-site linewidth is observed at either transition, in agreement with previous studies.[15,16]

Note that significant magnetic-field-induced electrical changes have been observed in $NbSe_3$ below 59 K, in fields of a few T.[6] However, these effects have consistently been observed only with the *b* axis perpendicular to the magnetic field, whereas for all results reported here the *b* axis was parallel to the field. Therefore Fermi-surface characteristics deduced in these studies can be assumed to apply to the zero-field configuration. The lack of NMR Knight-shift anomalies in studies at different fields[15,16] gives further evidence.

B. Spin-lattice relaxation

To measure relaxation, we determined the signal amplitude by integrating over the line for each site, where

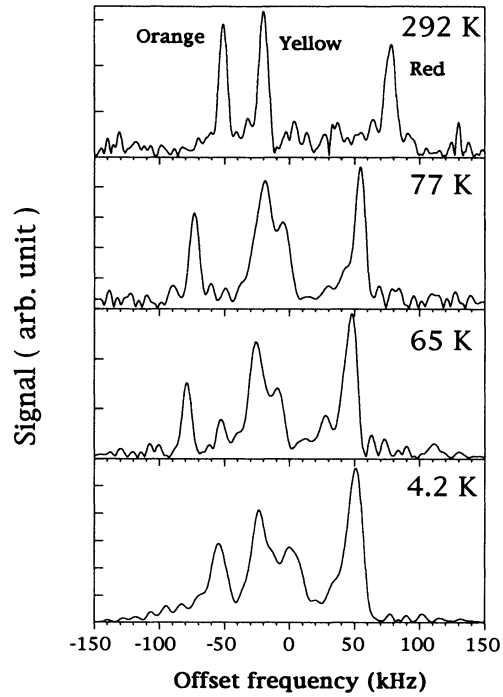

FIG. 1. Central-transition ^{93}Nb NMR spectra measured at temperatures bracketing the 145- and 59-K CDW transitions in $NbSe_3$. Measurements were taken at $H=8.975$ T, with crystal *b* axes parallel to the field. Frequency denotes the offset from 93.61 MHz. Identification with the three crystallographic sites is as shown.

the spectrum was obtained from echo FFT's of signal-averaged data. For the broadened yellow-site central line, we integrated the entire line. Finally the signals obtained at different temperatures were fitted to the appropriate theoretical recovery curve using a χ^2 method to

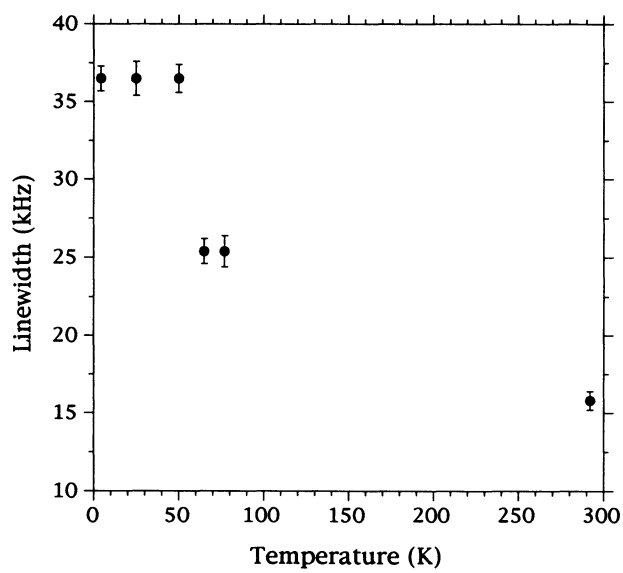

FIG. 2. Yellow-site central-transition NMR linewidth (FWHM) as a function of temperature, at 8.975 T, showing a sudden change for temperatures near the 59-K CDW phase transition.

optimize the curve fit. One such fit is shown in Fig. 3, where the theoretical curves are described below.

For the central transition, the spin-lattice relaxation is a multiexponential expression.[19,20] Three methods are used in our relaxation analysis for different temperatures. Standard inversion recovery using a composite inversion pulse[21] was applied for the room-temperature measurements. In this case the magnetization recovery has the form[20,22]

$$M(T)=M_0(1-0.012e^{-2Wt}-0.067e^{-12Wt}-0.185e^{-30Wt}-0.430e^{-56Wt}-1.306e^{-90Wt}) . \quad (1)$$

Here, $2W=(T_1)^{-1}$, and T_1 refers to the relaxation exponent observed when all transitions are saturated in NMR, by the conventional definition. Hence, a fit to Eq. (1) yields the single time T_1 for each site. Three parameters were adjusted in the fit: the T_1, the inversion efficiency, and the asymptote.

A modified method was used for 77 K, due to the relatively long relaxation time. We found numerical solutions to the rate equations for magnetic inversion recovery having T_{rep} not much longer than T_1. Here T_{rep} is the time between the measured echo and the next saturation pulse, during repetitive signal averaging. We can use a much shorter T_{rep} to significantly reduce the data-acquisition time. Numerical solutions were obtained using the symbolic-manipulation program MATHEMATICA, and while the exact curve was obtained, the corrections from Eq. (1) were small for $T_{rep} \geq T_1$.

Because of slow relaxation at 4.2 K, a steady-state method was applied, which is more efficient than inversion recovery, but rather complicated for quadrupole split spectra. We again used MATHEMATICA to determine the theoretical spin-lattice recovery curves for the steady state. In the steady-state experiment, echo measurement saturates the central transition periodically, but in the relaxation process all levels are affected so that the recovery curve is different from (1). In this case, an exact analytical multiexponential expression was derived, containing more than 50 exponential terms (too long to show here). An eight-echo Carr-Purcell-Meiboom-Gill[23,24] pulse sequence, which has one 90° pulse followed by a series of 180° pulses, was used for 4.2-K measurements. This sequence improves the signal-to-noise ratio and also gives near perfect saturation for each transition. Each echo was separately digitized and averaged, and all echo FFT's were added after multiplying by a weighting function equal to the T_2 decay function, to optimize the signal-to-noise ratio. The signal strength was then obtained by integrating over the echo FFT width for each site.

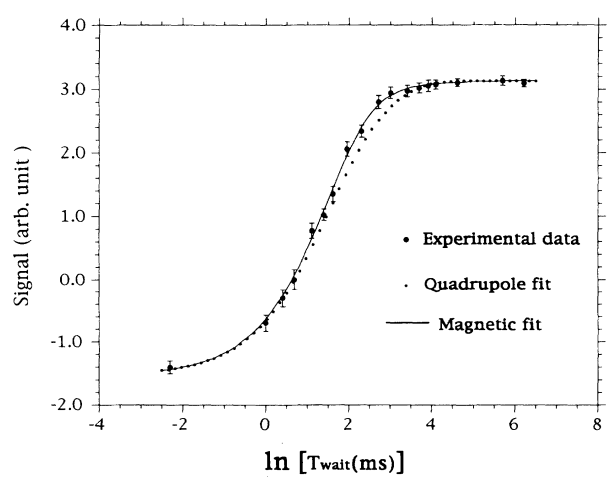

FIG. 3. Experimental relaxation data for the $NbSe_3$ orange-site central line, at 77 K, with the theoretical fits. Curves for the magnetic and quadrupole relaxation mechanisms are described in the text.

For the transition metals, spin-lattice relaxation involves several hyperfine coupling terms[19,20] including s-contact, core-polarization, and orbital interactions, and in exceptional cases magnetic dipole and electric quadrupole interactions with conduction electrons. Hyperfine coupling parameters are reasonably well established for niobium metal.[19] Based on well-established band structures, there is no contribution from s contact in $NbSe_3$. In addition, band calculations indicate that the terms $|\langle k,m|L^{\pm}|k',m'\rangle|^2$ are negligible because there is no d_{xz},d_{yz} mixture at the Fermi surface[9–11,14] in the undistorted configuration. This means that the orbital contribution goes to zero. We therefore assume in our analysis that core polarization is the dominant contribution to the relaxation, and it has the form[20]

$$1/T_1=2\gamma_n^2 hk[N(E_F)]^2 H_{cp}^2 T , \quad (2)$$

where T_1 is spin-lattice relaxation time, H_{cp} is the hyperfine core-polarization field, T is the temperature, $N(E_F)$ is the density of states, while γ_n is the gyromagnetic ratio. Interference terms[20] will not appear because there is essentially one orbital of importance, the d_{z^2} orbital. Also, the effect of electron-electron interactions on T_1 is generally small.[25]

Electric quadrupole interactions with unfilled shell electrons in some cases contribute to the spin-lattice relaxation, but for Nb, this should be small as illustrated by the result for ^{95}Mo in the same row.[25] Thus this process is disregarded in our analysis. The final T_1 figures for three sites at three temperatures, derived from fits to magnetic recovery curves as described above, are given in Table I. The uncertainties quoted in this table correspond to the 90% confidence level obtained from a χ^2 fit.

Additional contributions to T_1 may come from quadrupole coupling to atomic fluctuations. A standard phonon contribution is unlikely as the source of T_1 observed here, since the T dependence will be much stronger than actually observed (Table I).[26] However, further contributions can come from CDW fluctuations; this has been observed in NQR studies of $NbSe_3$ (Ref. 27) just below the 145-K transition, giving a peak in the relaxation rate that dies out quickly with reduced temperature. A comparison between T_1 data from Table I and preliminary nuclear quadrupole resonance results[27,28] shows no frequency dependence at 77 K, indicating against such a mechanism at this temperature. Furthermore, a least-squares fit of the 77-K relaxation data to a quadrupole curve (shown

TABLE I. ^{93}Nb NMR spin-lattice relaxation time (T_1) measured for each site in $NbSe_3$, at different temperatures, at $H=8.975$ T.

Temperature \ Site	Red site (II)	Orange site (I)	Yellow site (III)
292 K	67.3±2.4 ms	21±1 ms	12.6±0.7 ms
77 K	410±22 ms	165±9 ms	330±16 ms
4.2 K	26.6±1.8 s	23.5±1.35 s	18.7±1.2 s

in Fig. 3 for the orange site), is much less satisfactory than the magnetic fit. For this fit, the quadrupole relaxation parameters[29] were set so that $W_1=W_2=W$, appropriate to fluctuations of the well-established yellow-site crystal field.[28] In this case the solution has the form

$$M(t)=M_0(1-0.012e^{-2627Wt}-0.353e^{-2318Wt}-0.345e^{-1821Wt}-0.807e^{-944Wt}-0.482e^{-330Wt}) . \quad (3)$$

III. DENSITIES OF STATES AND ANALYSIS

Using the core-polarization model, the density of states from Eq. (2) for each site at room temperature, 77 K, and 4.2 K is given in Table II. We used a core-polarization hyperfine field (H_{cp}) equal to -0.18×10^6 G, which is the experimental value for $NbSe_2$.[30] Theoretical values for Nb metal range from -0.14×10^6 to -0.21×10^6 G;[19,31,32] choosing values in this range will scale $N(E_F)$ accordingly, although relative changes at the transitions will be unaffected. Our results show that $N(E_F)$ is reduced by 43% when the temperature changes from 292 to 77 K, and is further reduced by 53% when the temperature drops from 77 to 4.2 K, which is consistent with the opening of Fermi-surface gaps due to the two CDW transitions. Previous estimates from resistivity[5,33] had approximately 20–30% of the Fermi surface destroyed by the 145-K transition and 60–70% of the remaining Fermi surface destroyed by the 59-K transition.

The total $N(E_F)$ from Table II, 2.43 states/(eV Nb atom), is also comparable to the total $N(E_F)$ calculated by Shima,[11] 1.30 states/(eV Nb atom), for room temperature, although the difference is too large to attribute to uncertainty of H_{cp}. However, our results provide strong evidence that the red site is neither equivalent to the orange site nor insulating, which have been the two previous theoretical predictions.[11,14]

Comparing the 77-K to room-temperature results, we can see that the yellow site exhibits the largest $N(E_F)$ change due to the 145-K phase transition, which is consistent with previous experimental and theoretical results. However, the density of states at all sites is affected. Clearly, the band associated with that transition is not as spatially confined as had been believed.

For the low-temperature transition case, our results indicate the largest $N(E_F)$ change for the orange site between 77 and 4.2 K. However, again all three sites participate to some extent. As described above, the yellow line has a sudden change in linewidth near 59 K (Fig. 2). Enhanced broadening may result from the condensation of the free electrons that screen the electric-field gradient, without a change in the magnitude of the high-temperature CDW, which is consistent with the x-ray scattering-result.[34] Thus, some of the electrons that condense at low temperatures must come from the yellow site. Our total $N(E_F)$ for 4.2 K, 0.65 states/(eV Nb atom), is somewhat larger than that of Shima's[11] 0.41 states/(eV Nb atom), a trend also seen at room temperature.

A contribution to the T_1 due to vibration modes at 4.2 K cannot be ruled out as it was for 77 K. This would make the $N(E_F)$ in Table II somewhat smaller. Low-energy fluctuation has been evidenced in the specific heat,[35] but these are unlikely to be important at 90 MHz. Furthermore, CDW fluctuations cannot be effective on the red-site T_1 since CDW broadening is absent for that site. Thus, such terms must have a small effect on the T_1.

Note, however, that our analysis assumed no orbital contribution, based on band-structure calculations for the undistorted configuration. Rough agreement between our total $N(E_F)$ and that of Shima[11] tends to confirm this argument. However, symmetry change below the CDW transition may modify the band structure sufficiently to add an orbital term (e.g., adding d_{xz} and d_{yz} contributions), lowering $N(E_F)$ by a small amount.

It is difficult to reconcile, though, the much smaller $N(E_F)$ implied by recent specific-heat measurements.[35] The new value of $\gamma\leq8$ erg g^{-1} K^{-2} implies $N(E_F)$ not exceeding 0.12 states/(eV Nb atom) at low temperature. So the density of electrons remaining at low temperature remains somewhat uncertain. We note, however, that strong 4.2-K relaxation is seen for all three sites, presum-

TABLE II. Fermi-level densities of states for each Nb site in $NbSe_3$, in states/(eV Nb atom), deduced from the NMR T_1.

Temperature \ Site	Red site (II)	Orange site (I)	Yellow site (III)	Total
292 K	1.43	2.55	3.30	2.43
77 K	1.13	1.78	1.25	1.39
4.2 K	0.60	0.64	0.71	0.65

ably implying that multiple electron-hole pockets remain at this temperature, rather than the simple picture of one remaining pocket.

In a previous non-site-selective NMR relaxation experiment,[22] consistently shorter T_1 values for 77 and 4.2 K were reported. In our study, we see no sign of frequency dependence to the T_1, as seen in that study. It is possible that the additional relaxation was due to characteristics of the previous sample.

Additionally, Knight-shift measurements[16] have provided a rough quantitative measurement of the changes in the density of states caused by CDW transitions. The previous analysis assumed that the red site is insulating, with zero spin susceptibility, as originally believed.[8] Our measurements provide considerably more detail, since for T_1 evaluation, differences between large core dimagnetism, Van Vleck, and core-polarization terms are not involved. Our revised picture of the per-chain electron configuration, though, is consistent with the Knight-shift data and estimates that roughly half of the Fermi surface at both the yellow and orange sites is destroyed at the corresponding transition.

Finally, we address the lack of modulation on the red site at low temperature. In our study, as well as previous studies,[15,16] no linewidth change was observed for the red site, although some $N(E_F)$ change was observed. Thus the apparent conflict with STM (Ref. 17) remains. A possible resolution for this conflict involves a low-temperature CDW located on the red-site seleniums as well as orange-site metal atoms. The effect on the red-site Nb resonance could then be small. Note that the red-site Se-Se antibonding orbitals are predicted to lie just below the Fermi level.[11,14] To have some CDW density in these orbitals requires an upward energy shift for that band, possibly caused by the CDW distortion itself.

IV. CONCLUSIONS

We have measured the Nb-site T_1 in $NbSe_3$ and thereby resolved the temperature dependence of metallic electrons per chain. We present a microscopic picture of the two CDW transitions, showing large changes in the density of states for the yellow and orange sites due to the 145- and 59-K transitions, respectively. CDW broadening is also exclusive to these two sites, as previously observed. Yet the third site (red site) does exhibit significant density-of-states changes. We find that band-structure calculations have successfully predicted the main features, but certain aspects, particularly the nature of the pockets remaining at low temperatures, remain unresolved.

ACKNOWLEDGMENTS

We gratefully acknowledge the interactions with Charles P. Slichter, Zhiyue Wang, and Bryan H. Suits that led to this work. Also, we thank Jin Lu, James Chepin, and Xun Ge for their contributions to the construction of the spectrometer.

[1]G. Grüner, Rev. Mod. Phys. **60**, 1129 (1988).
[2]Alain Meerschaut and Jean Rouxel, in *Crystal Chemistry and Properties of Materials with Quasi-One-Dimensional Structures,* edited by J. Rouxel (Reidel, Dordrecht, 1986), p. 205.
[3]Pierre Monceau, in *Physics and Chemistry of Materials with Low-dimensional Structures, Part II,* edited by Pierre Monceau (Reidel, Dordrecht, 1985), p. 139.
[4]Joseph H. Ross, Jr. and Charles P. Slichter, in *Nuclear Spectroscopy of Charge-Density-Wave Systems,* edited by T. Butz (Riedel, Dordrecht, in press).
[5]N. P. Ong, Phys. Rev. B **18**, 5272 (1978).
[6]R. V. Coleman, *et al.*, Phys. Rev. B **41**, 460 (1990).
[7]Robert A. Scott, *et al.*, Inorg. Chem. **25**, 1461 (1986).
[8]J. A. Wilson, Phys. Rev. B **19**, 6456 (1979).
[9]D. W. Bullett, J. Phys. C **12**, 277 (1979).
[10]Roald Hoffmann *et al.*, J. Solid State Chem. **34**, 263 (1980).
[11]Nobuyuki Shima, J. Phys. Soc. Jpn. **52**, 578 (1983).
[12]Nobuyuki Shima and Hiroshi Kamimura, in *Theoretical Aspects of Band Structures and Electronic Properties of Pseudo-One-Dimensional Solids,* edited by Hiroshi Kamimura (Reidel, Dordrecht, 1985), p. 231.
[13]Enric Canadell and Myung-Hwan Whangbo, Inorg. Chem. **25**, 1488 (1986).
[14]E. Canadell *et al.*, Inorg. Chem. **29**, 1401 (1990).
[15]Joseph H. Ross, Jr., Zhiyue Wang, and Charles P. Slichter, Phys. Rev. B **41**, 2722 (1990).
[16]F. Devreux, J. Phys. (Paris) **43**, 1489 (1982).
[17]Zhenxi Dai, C. G. Slough, and R. V. Coleman, Phys. Rev. Lett. **66**, 1318 (1991).
[18]A. Meerschaut and J. Rouxel, J. Less Common Met. **39**, 197 (1975).
[19]Y. Yafet and V. Jaccarino, Phys. Rev. **133**, 1630 (1964).
[20]A. Narath, Phys. Rev. **162**, 320 (1967).
[21]A. J. Shaka, Chem. Phys. Lett. **120**, 201 (1985).
[22]Shinji Wada, Ryozo Aoki, and Osamu Fujita, J. Phys. F **14**, 1515 (1984).
[23]H. Y. Carr and E. M. Purcell, Phys. Rev. B **94**, 630 (1954).
[24]S. Meiboom and D. Gill, Rev. Sci. Instrum. **29**, 688 (1958).
[25]Albert Narath and Donald W. Alderman, Phys. Rev. **143**, 328 (1966).
[26]Robert Lee Mieher, in *Semiconductors and Semimetals,* edited by R. K. Willardson and Alber C. Beer (Academic, New York, 1966), p. 141.
[27]B. H. Suits and C. P. Slichter, Phys. Rev. B **29**, 41 (1984).
[28]Joseph H. Ross, Jr., Ph.D. thesis, University of Illinois at Urbana-Champaign, 1986.
[29]E. R. Andrew and D. P. Tunstall, Proc. Phys. Soc. London **78**, 1 (1961).
[30]C. Berthier, D. Jerome, and P. Molinie, J. Phys. C **11**, 797 (1978).
[31]T. Asada, K. Terakura, and T. Jarlborg, J. Phys. F **11**, 1847 (1981).
[32]H. Ebert, H. Winter, and J. Voitländer, J. Phys. F **16**, 1133 (1986).
[33]Masayuki Ido *et al.*, J. Phys. Soc. Jpn. **59**, 1341 (1990).
[34]R. M. Fleming *et al.*, Phys. Rev. B **30**, 1877 (1984).
[35]K. Biljaković, J. C. Lasjaunias, and P. Monceau, Phys. Rev. B **43**, 3117 (1991).